6

USE OF EARTH OBSERVATION TO SUPPORT URBAN MODELLING PARAMETERIZATION IN BRIDGE

Constantinos Cartalis[1], Marina Stathopoulou[1], Zina Mitraka[2] and Nektarios Chrysoulakis[2]

[1]UNIVERSITY OF ATHENS AND [2]FOUNDATION FOR RESEARCH AND TECHNOLOGY - HELLAS

Introduction

Urban studies conventionally use environmental and geographic information so as to depict the state of the urban environment, the characteristics of the urban landscape, the changes that have taken place in the course of time, the pressures on the urban area and the potential of varying techniques and technologies to ameliorate the thermal environment (Grimmond et al. 2010; Santamouris et al. 2011). Such information needs to be spatially and temporally dense, a fact which implies the need for monitoring networks or special experiments having the capacity to sufficiently reflect the area under investigation. Despite improvements in our understanding of urban processes and their impact on quality of life of city dwellers, few cities or urban agglomerations operate monitoring networks that may be considered sufficient.

As discussed in the next chapter, atmospheric models are increasingly employed to improve the understanding of processes that are related to local scale climate and air quality, the urban heat island and meso-scale circulations related to surface land cover and characteristics. Such processes are strongly influenced by the energy and momentum exchange between the atmosphere and the underlying surface; hence, the simulation of these processes depends on the accurate characterization of the surface properties. Information on surface physical properties (e.g. albedo, emissivity) and morphology (e.g. ground elevation, building height and geometry characteristics) is generally needed. Update-to-date information on these parameters can be provided by the current Earth Observation (EO) satellites and is expected to be improved in the near future. This chapter presents the potential of the current EO systems to support surface parameterization in model simulations that were performed in BRIDGE (Chrysoulakis et al. 2013a), and also providing some examples of such satellite derived products for the case study of Athens.

To many urban planners EO is providing a reliable alternative to conventional techniques (Esch et al. 2013). Yet considerable discussion is taking place on the real capacity of EO to support urban studies, including urban modelling. Such discussion mostly relates to the resolution (temporal, spatial and spectral) of satellite images. If the spatial resolution is low, studies may reflect inaccuracies, especially in the area of land use/cover changes. On the contrary, if the spatial resolution is high, the load of exploitable information may highly exceed the respective load of ground data. In addition, temporal and spatial resolutions of a satellite image are anti-correlated, meaning that the better the spatial resolution, the worse the temporal one, and vice versa. When discussing satellite images, spectral resolution also needs to be explored as the combined use of varying spectral channels may provide invaluable products for the state of the urban environment and the respective processes. For instance, although the study of many urban applications is based on images in the visible and near infrared parts of the spectrum, satellite images in the thermal infrared have an excellent potential in terms of supporting urban microclimatic studies.

In terms of urban modelling, different models are used, from meso-scale air quality models to urban canopy models. As discussed in more detail in Chapter 7, the modelling approach of BRIDGE was based on the cascade modelling technique (large to local scale) and includes the following steps: a) energy and water fluxes were measured and modelled at local scale; b) fluxes of carbon and pollutants were also modelled and their spatio-temporal distributions were estimated; c) fluxes were dynamically simulated in a 3D context by using state-of-the-art numerical models; and d) outputs of the above models resulted in indicators, which defined the state of the urban environment and were incorporated into the BRIDGE Decision Support System (DSS).

EO supported the models used in BRIDGE with detailed (spatially and temporally) information for such parameters as Land Surface Albedo (LSA), Land Surface Emissivity (LSE) and Land Surface Temperature (LST). It also provided topographic data in support of the development of Digital Elevation Models (DEMs), as well as estimates of the Aerosol Optical Thickness (AOT), i.e. a parameter considered essential for surface LSA calculations. Finally, it provided valuable information on land use/cover; such information, once provided in adequate resolution, allows the detection of changes which may be attributed to urban processes and patterns. To this end, the potential of EO is considered important especially taking into consideration the developing wealth of satellite sensors and the overall improvement in their spatial, temporal and spectral resolutions. Below, a concise description regarding the methodology applied for each of the above parameters is given, along with some examples from the case study of Athens, as promoted within the BRIDGE project.

Satellite derived LSA

Satellite derived LSA products are used as inputs in meso-scale model simulations. LSA can be estimated from white-sky (completely diffuse) and black-sky (direct beam) albedo products as retrieved from Moderate Resolution Imaging Spectroradiometer (MODIS) observations for each elementary (dependent on the spatial resolution of the sensors) surface (Schaaf et al. 2002). It is noted that the spectral albedo is not a true surface property, but rather a characteristic of the coupled surface–atmosphere system. However, both black-sky and white-sky albedos are true surface properties and correspond to the limiting cases of point source and completely diffuse illumination. MODIS observations do not directly measure LSA; to this end spectral albedo is derived by directional integration of land surface reflectance recorded at the sensor, and is therefore dependent on the Bidirectional Reflectance Distribution Function (BRDF), which describes the dependency of reflectance on view and solar angles.

A directional sampling of surface reflectance from sensors such as MODIS can only be obtained by the accumulation of sequential observations over a specified time period. A 16-day period (or more) reflects a trade-off between the sufficiency of angular samples and the stability of surface reflectivity. These directional observations can be coupled with semi-empirical models to describe the BRDF and integrals necessary to provide spectral albedos. As discussed by Lucht et al. (2000), the BRDF can be expanded into a linear sum of terms (the so-called kernels), characterizing different scattering modes (isotropic, volumetric and geometric). The MODIS BRDF/albedo algorithm makes use of a kernel-driven, linear BRDF model which relies on the weighted sum of an isotropic parameter and two kernels (volumetric and radiometric) of viewing and illumination geometry to determine reflectance (Schaaf et al. 2002).

The black-sky albedo, as well as the white-sky albedo, are computed using polynomial expressions of the kernel weights, as described by Schaaf et al. (2002). The diffuse component can be expressed as a function of wavelength, optical depth, aerosol type and terrain contribution. Therefore, for partially diffuse illumination actually occurring, the spectral albedo may be approximated as a linear combination of the limiting cases. For this approximation, the fraction of diffuse radiation should be calculated; its calculation is straightforward as a function of solar zenith angle and AOT.

If Lambertian conditions are assumed, LSA may also be approximated from satellite images of high spatial resolution. Using the band image data of Thematic Mapper (TM) of Landsat as recorded in the visible, near-infrared and mid-infrared spectral channels, the total shortwave albedo (0.25–5.1 μm), the visible albedo (0.4–0.7 μm) and the near-infrared albedo (0.7–5.0 μm) can be calculated at the spatial resolution of 30 m. In particular the processing technique includes:

- estimation of the incoming spectral radiative fluxes at the top of the atmosphere,
- atmospheric correction of the image data,
- correction of the incoming fluxes for the orientation of the surface and for the anisotropic reflection by the surface,
- conversion of the estimated surface leaving spectral radiance to surface spectral reflectance,
- conversion of the surface spectral reflectance to surface spectral albedo,
- conversion of the surface spectral albedo to broadband surface albedo as per Liang (2001).

For example, in the Athens case study, besides the MODIS derived LSA time series used in meso-scale modelling parameterization, LSA was also derived from a high-spatial resolution satellite image acquired over metropolitan Athens from Landsat 5, under cloud free atmospheric conditions. The processing technique followed the above steps. The resulted shortwave albedo is shown in Plate 4. A zonal analysis of the product, leads to the conclusion that the most densely built areas of Athens exhibit a mean shortwave albedo value of 14.7 per cent, whereas all types of urbanized surfaces of the city can be represented by a mean value of 15.85 per cent (Stathopoulou et al. 2009).

Satellite derived LSE

Satellite derived LSE products are used in meso-scale models simulations. Daily emissivity maps (MODIS Level 2 emissivity product) are available as global maps at 1 km spatial resolution. The classification-based emissivity method proposed by Snyder et al. (1998) is used as developed with the linear BRDF models. Such models utilize spectral coefficients derived from laboratory measurements (Salisbury & D'Aria 1992, 1994: Salisbury et al. 1994: Snyder et al. 1997) of material samples. They also use structural parameters as derived from approximate descriptions of the cover type (Snyder & Wan 1998). LSE can be also be estimated with high resolution satellite data taking into account the 'mixed pixels' problem and the emissivity angular anisotropy (Mitraka et al. 2012).

Another methodology is exemplified in the following example: LSE was derived at spatial resolution of 30 m following the processing of three Landsat TM images as acquired over metropolitan Athens during the warm season of the year. For each of these images, effective LSE in the 10–12 μm waveband was derived applying the algorithm proposed by Caselles et al. (1991) and using a mean thermal emissivity value of 0.93 for the urbanized areas of Athens and a mean value of 0.98 for the vegetated surfaces (Stathopoulou & Cartalis 2007a). Then a composite LSE image was produced as a result of the overlay of LSE images and considering a mean LSE value for each pixel. In this way, a mean seasonal LSE image of Athens was produced (Plate 5), showing lower LSE values in the central and NW suburbs of Athens as compared to the N and NE ones, a fact which implies the presence of less vegetation and green open spaces in these areas.

LST and surface urban heat island

LST is a key parameter for mapping surface urban heat islands (SUHIs) and understanding the state of the thermal environment, including energy fluxes. It can be retrieved from thermal infrared image data at varying temporal and spatial resolutions (Prata et al. 1995: Sobrino & Jiménez-Muñoz 2005), with the principal preconditions for the retrieval being the correct estimation of the atmospheric effects and of LSE.

On the basis of LST, information about the SUHI characteristics of a city can be obtained, such as development and spatial pattern (heat island or heat sink), growth and evolution (SUHI area in km^2), and intensity (LST difference observed between urban areas and the surrounding countryside).

In general, the processing steps for the estimation of LST and SUHI from satellite data are:

- Selection of satellite data and pre-processing (radiometric correction, cloud masking, geometric correction and projection to a standard geodetic system).
- Definition of methodology/technique for the analysis of thermal infrared image data to estimate LSE and LST. Special attention needs to be given, on the basis of land cover, to the distinction of urban to non-urban areas, as well as to the distinction of the urban areas as a function of the optical and thermal properties of commonly used building and paving materials.
- Application of image processing methodologies/techniques to satellite imagery with the final stage being the classification of the thermal surface pattern of the urbanized centres and the development of thermal maps of the urban areas.
- Application (potentially) of remote sensing downscaling techniques for low resolution data for selected cases.
- Use of high resolution satellite data in the identification of 'hot spot' events within the urban areas under study.
- Estimation of LST gradients within the urban areas and detection/measurement of the SUHI, including its extent and intensity.
- Link of LST/SUHI to land use/cover, physical interpretation and statistical analysis.
- Validation of results based on error analysis and determination of classification accuracies.

Many SUHI studies focus on the use of polar orbiting satellites that have adequate spatial resolution (~1 km) and daily revisiting capabilities, such as MODIS. For example, Hung et al. (2006) used MODIS data to perform a comparative study of the SUHIs of eight megacities in Asia. Besides MODIS data, they also utilized high spatial resolution Landsat satellite images to derive land cover information and to relate SUHI patterns to surface characteristics. The researchers adopted the Gaussian method proposed by Streutker (2002) and measured the spatial extents and intensities of the SUHIs of the eight megacities. The diurnal and seasonal patterns of the SUHIs revealed that all cities exhibited significant heat islands. Likewise, many researchers (Dousset & Gourmelon 2003; Stathopoulou et al. 2004; Tomlinson et al. 2012) have demonstrated that the use of low resolution data in large urban agglomerations may provide solid information on the presence, extension and differentiation of LST and SUHI. In practice, data from satellites with high revisit time such as MODIS or AVHRR, support the monitoring of the SUHI intensities at a frequent basis as well as the retrieval and mapping of the thermal inertia of the urban landscape; the latter supports the understanding of the roles that individual components of the city (such as parks, industrial complexes, etc.) play in the thermal patterns of the city (Voogt & Oke 1998). This requirement is particularly important if the link between SUHI intensity and air pollution is to be explored (Lo & Quattrochi 2003), or if satellite-derived LST is used to calculate energy parameters, such as the cooling degree days (Stathopoulou et al. 2006) or bioclimatic parameters, such as the thermal discomfort index (Stathopoulou et al. 2005).

LST can be also estimated with the use of satellite imagery of spatial resolutions from 60, to 90 to 120 m. Such imagery may be highly beneficial to detect 'hot spots' within urban areas or to examine in better spatial detail findings from 1 km resolution satellites. This requirement is of particular importance if the study area reflects a city of moderate size (Stathopoulou et al. 2004), or a region of particular interest within a city (Nichol 1996). At the same time, such imagery faces the problem of limited temporal resolution (revisit time of the order of 16 days), a fact which narrows the operational character of the application. It should be mentioned that the potential of downscaling techniques as applied to low spatial resolution satellite data (Stathopoulou & Cartalis 2009) has already been examined, with promising results in terms of the capacity of the methodology developed to adequately reflect the radiometric information at an improved spatial resolution. Jiménez-Muñoz & Sobrino (2003) have developed a generalized split-window algorithm for the retrieval of LST that can be applied to all thermal sensors characterized with a Full-Width Half-Maximum (FWHM) of around 1 μm. The main advantage of this algorithm is that it can be applied to different thermal sensors using the same equation and coefficients.

An LST estimation methodology is exemplified in the following example, where summertime Landsat images over the metropolitan Athens area were analysed: following the calibration process of the thermal channel image data, the generalized single-channel algorithm (Jiménez-Muñoz & Sobrino 2003) was applied. The algorithm requires knowledge of LSE for the application area, as well as the atmospheric water vapour content for the observation day. Therefore, the algorithm was applied using LSE values by land cover (Stathopoulou & Cartalis 2007b) and a mean value of water vapour content per month as measured from radiosonde data in Athens (Chrysoulakis & Cartalis, 2002). As shown in Figure 6.1, the mid-morning summertime LST spatial profile demonstrates the development of a negative SUHI (heat sink), with the extended dry surfaces of bare soil and low vegetation in the surrounding rural areas presenting higher LST values than the urbanized surfaces of the Athens basin. The latter, as characterized by lower sky view factor and higher thermal capacity, exhibits lower warming rate from incident solar radiation compared to rural areas at the periphery of the city (Stathopoulou & Cartalis 2007a).

Land use/cover

In order to determine the intensive interactions between humans and the environment in the cities, especially in the metropolitan areas and their peripheries, as well as to determine and monitor the main characteristics of change, Land Use/Land Cover (LULC) monitoring and extracting LULC type is important (Qian 2007). Urban land cover units can be distinguished by their characteristic pattern of built and open spaces, which form the background matrix of the city, whereas the different materials can be distinguished by their characteristic spectral response (Chrysoulakis et al. 2013b; Herold et al. 2003; Pauleit & Duhme 2000). Land cover units result from past and present human activities and form relatively stable features lasting in time. Furthermore, land cover units are the product of land use and development plans. Delineating these units leads to an assessment of past and current city planning decisions. In addition, planning concepts such as mixed housing areas in closed block buildings versus housing in multi-story high rise buildings can be evaluated. Land cover units also have a characteristic land use associated with them (Weber et al. 2005; Chorianopoulos et al. 2010).

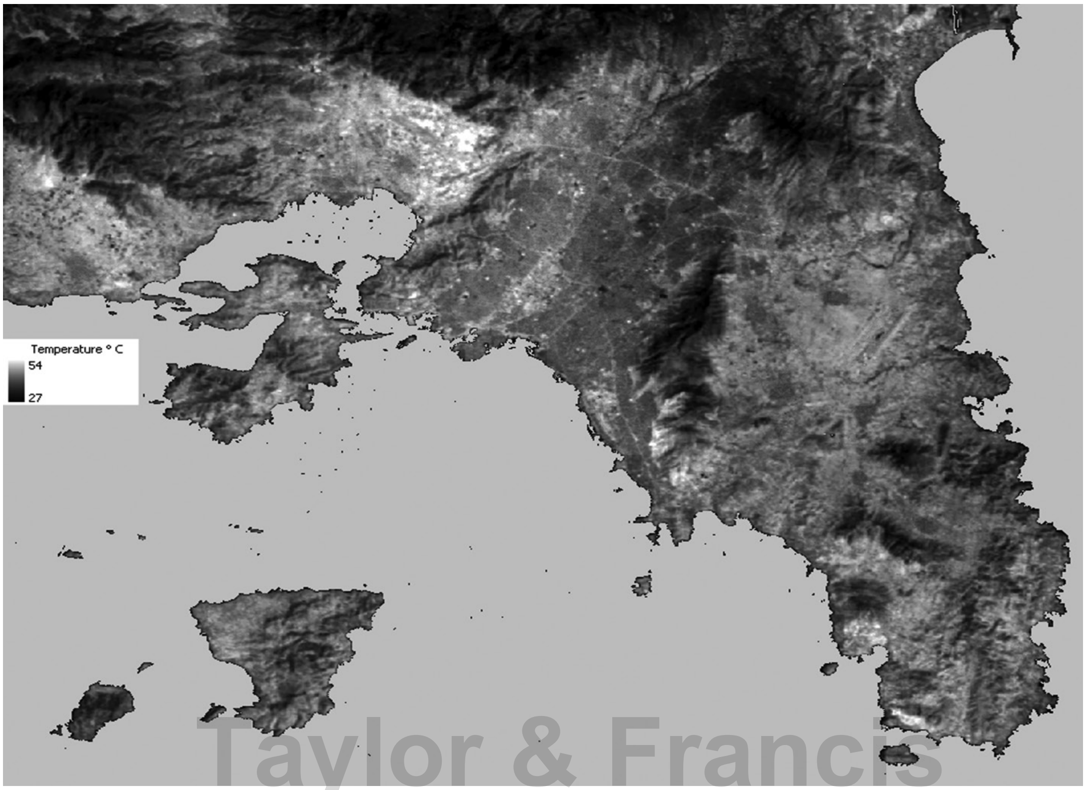

FIGURE 6.1 Surface temperature in Athens (daytime analysis) based on Landsat observations and auxiliary spatial data

Several classification and segmentation methods have been developed for the processing of satellite data for land cover/land use applications. Although supervised classification can be used for LULC classification purposes, the 'mixed pixel' problems can affect the results because of the nature of the classificatory criteria (Enderle & Weih 2005; Bhaskaran et al. 2010). The object-oriented classification method can be more successful than the pixel-based methods (Whiteside & Ahmad 2005; Chena et al. 2009; Chrysoulakis et al. 2013b) as it creates segments from image pixels which includes homogeneous, spatially contiguous regions.

The object-based classification process of satellite images is based on object-oriented software. Object-oriented software requires first segments which have to be created by pre-set homogeneity criteria. The scale, colour and form parameters are used to create homogeneous segments from pixels. These parameters are defined by the user in an empirical manner, whereas the scale parameter affects the heterogeneity of the pixels. The colour parameter defines balance between the homogeneity of a segment's colour and the homogeneity of its shape. The smoothness of an object's border with its compactness can be balanced with the form parameter. The segmentation process has been explained in detail by Baatz & Schäpe (2000). To achieve expected results, scale factor and other segmentation criteria are chosen empirically and interactively to demonstrate the morphology of the objects (Ranasinghe 2008).

Satellite images of high spatial resolution are required to map the LULC of the city giving emphasis to differentiating between urban and non-urban uses: 1) high-density urban use; 2) low-density urban use; 3) cultivated/exposed land; 4) cropland or grassland; 5) forest; and 6) water. The LULC change analysis is performed on the basis of statistics (coverage percentage) extracted from the produced land use/cover maps of the city area.

The methodology used to map the dynamics of urban growth in a study area includes pre-processing of high resolution images before urban feature extraction and the use of orthorectified products as reference data sets to geometrically correct the images. The brightness normalization method proposed by Wu (2004) can be applied to handle difficulties in quantifying urban composition. Although urban components show significant spectral differences (e.g. dark and bright soil), they share common characteristics. The normalization technique is used to highlight the shape information, while minimizing the effects of absolute reflectance values, by reducing the spectral variations between pure land use types.

Satellite derived DEMs

Advanced Spaceborne Thermal Emission and Reflection Radiometer (ASTER) stereo imagery has been used in BRIDGE for DEM generation at city and regional scales, for all BRIDGE case studies. For the production of a DEM from optical satellite data, the respective satellite sensors should have stereo coverage capabilities (Toutin 2001). The methods for applying stereoscopy to push-broom scanners generally use the rigorous photogrammetric solution (collinearity and coplanarity conditions for the conic perspective of a single image line), but also take into account the displacement of the satellite (cylindrical perspective) to link the equations between themselves (Toutin 2004). Since the parameters of neighbouring lines are highly correlated and satellite positions and attitude can be computed from on-board recording systems, the mathematical equations can be reduced to a minimum of eight to ten unknowns, depending on the mathematical development and the algorithm implementation of the solution. A stereo matching process to extract elevation parallaxes is applied (Toutin 2008). In particular, the basic characteristics of stereoscopy and its application to the ASTER for DEM generation have been recently reviewed by Toutin (2008). ASTER consists of three separate instruments subsystems, each operating in a different spectral region, using separate optical system. These subsystems are the Visible - Near Infrared (VNIR), the Short-Wave Infrared (SWIR) and the Thermal Infrared (TIR). The spatial resolution varies with wavelength: 15 m in the VNIR, 30 m in the SWIR and 90 m in the TIR. The VNIR subsystem consists of two telescopes – one nadir looking with a three band detector (Channels 1, 2 and 3N) and the other backward looking (27.7° off-nadir) with a single band detector (Fujisada 1994; Abrams 2000). The data products provided by the ASTER have been summarized by Yamaguchi et al. (1998).

The vertical accuracy of a DEM product is assessed using Global Positioning System (GPS) measurements. Elevation accuracy is generally of the order of the system instantaneous field of view (or approximately the pixel spacing), also taking into account the Base to Height ratio (B/H). The theoretical accuracy of ASTER DEMs is therefore governed by the accuracy of the control data, the B/H and the matching. Since an error of $\pm$ 0.5–1 pixel or better for the parallax measurements in the automated matching process has been achieved with different data sets from other sensors, the potential relative accuracy for the elevation with the ASTER stereo data (B/H = 0.6, pixel spacing of 15 m) can be of the order of 12–25 m or better depending of the type of terrain. In addition, the accuracy of the DEM will also depend on the geometric parameter calibration, as well as the accuracy of the ephemeris and attitude data for computing the direct georeferencing.

The generation of a DEM for the broader Athens area using ASTER stereo-pairs is now briefly described: ASTER Level 1A data was projected to the map of Athens using the radiometric calibration and geometric correction coefficients for resampling (Fujisada 1998). Auxiliary and validation data sets for the study area include contour lines and shoreline digitized from 1:50.000 topographic maps, GPS measurements and the road network. The methodology for the production of DEM as described in Chrysoulakis et al. (2004a, b) and Nikolakopoulos et al. (2006) was applied to extract a high resolution (15 m pixel) ASTER DEM that was further used to orthorectify the respective ASTER multispectral imagery.

Next, virtual images were created using the respective VNIR and SWIR channels, as well as the extracted DEM. As a result, multispectral orthorectified images were created, each containing the respective DEM as a separate pseudochannel. In practice two mosaics were initially created: one for the DEM pseudochannels and one for the VNIR and SWIR channels of each image. In the former case, the radiometric values of each DEM were retained and a bilinear interpolation resampling method is used. In the latter case, the colour balancing and histogram matching functions were used and the radiometric values of VNIR and SWIR channels are slightly modified, ensuring the colour homogeneity of all scenes. The two mosaics were finally merged to one master mosaic covering the broader area of Athens. This mosaic was finally fine-tuned using the road network vectors of the area. In this way the plannimetric (xy) error was corrected to $\pm$ 0.5 pixel root mean square deviation (RMSE) using a 2D transformation, resulting in an planimetric accuracy of the corrected DEM better than 15 m. The produced DEM is shown in Plate 6.

CONCLUSIONS

A main conclusion is that EO is considered a valuable tool for urban modelling, as it can provide valuable spatial and temporal information regarding the topography and the LULC types of the study areas, as well as of such parameters as LSA, LSE, LST and AOT, used to parameterize atmospheric models at regional and local scales in BRIDGE. The combined use of satellite data in various spectral regions is also beneficial as the derived urban characteristics (land use/cover, vegetation cover) provide considerable insights with respect to the presence, the intensity and variability of the SUHI. Results can be further improved from the combined use of ground data and can also be used as the starting point for the estimation of such products as the thermal comfort index, or the cooling degree days.

Disadvantages do exist and relate mostly to the spatial and temporal resolutions of satellite images as well as to the knowledge of the properties of the emitting surfaces. In particular, urban studies which need satellite images of high temporal resolutions (order of hours), correspond to low spatial resolutions (order of 1 km), a fact which may be considered highly confining for detailed results (Stathopoulou & Cartalis 2007b). In the event that satellite images of medium resolution are used instead (120–250 m), the respective temporal resolution drops considerably (from 2–3 days to 16 days). However, given that urban studies focus on phenomena that in the long run reflect timescales exceeding those of hours or even days, such (temporal and spatial) resolutions may be considered adequate for large urban agglomerations. Problems do arise, however, in smaller urban areas as low or medium spatial resolutions may lead to only a few pixels of exploitable information. Problems also arise in the examination of the daily variation of microclimatic parameters, as limited information of high spatial resolution is available from satellite night passes. The latter may be considered the most pronounced drawback in terms of existing satellite sensors/missions, especially if the scope of study reflects the state of the thermal environment.

Overall the potential of EO for urban modelling parameterization is considered highly important, especially taking into consideration the wealth of existing satellite sensors and the forthcoming satellite missions (e.g. Sentinels) combined with the lack of extended and adequately operated ground monitoring networks. The potential is further enhanced in the event of cities of large size or cities falling in the category of 'mega cities'.

References

Abrams, M. (2000). ASTER: data products for the high spatial resolution imager on NASA's EOS-AM1 platform. *International Journal of Remote Sensing*, 21, 847–861.

Baatz, M., & Schäpe, A. (2000). Multiresolution Segmentation: an Optimization Approach for High Quality Multi-Scale Image Segmentation. In: Strobl, J., Blaschke, T., Griesebener, G. (Eds.), Angewandte Geographische Informationsverarbeitung XII. Beiträge zum AGIT-Symposium (Salzburg, Austria), Herbert Wichmann Verlag, Kahrlsruhe, pp. 12–23.

Bhaskaran, S., Paramananda, S., & Ramnarayan, M. (2010). Per-pixel and object-oriented classification methods for mapping urban features using Ikonos satellite data. *Applied Geography*, 30, 650–665.

Caselles, V., Lopez Garcia, M. J., Melia, J., & Perez Cueva, A. J. (1991). Analysis of the heat island effect of the city of Valencia, Spain through air temperature transits and NOAA satellite data. *Theoretical and Applied Climatology*, 43, 195–203.

Chena, M., Sua, W., Lia, L., Zhanga, C., Yuea, A., & Lia, H. (2009). Comparison of pixel-based and object-oriented knowledge-based classification methods using SPOT5 imagery. *WSEAS Transactions on Information Science and Applications*, 3, 477–489.

Chorianopoulos I., Pagonis T., Koukoulas S., & Drymoniti S. (2010). Planning, competitiveness and sprawl in the Mediterranean city: the case of Athens, *Cities*, 27, 249–259.

Chrysoulakis, N., Lopes, M., San José, R., Grimmond, C. S. B., Jones, M. B., Magliulo, V., Klostermann, J. E. M., Synnefa, A., Mitraka, Z., Castro, E., González, A., Vogt, R., Vesala, T., Spano, D., Pigeon, G., Freer-Smith, P., Staszewski, T., Hodges, N., Mills, G., & Cartalis, C. (2013a). Sustainable urban metabolism as a link between bio-physical sciences and urban planning: the BRIDGE project. *Landscape and Urban Planning*, 112, 100–117.

Chrysoulakis, N., Mitraka, M., Stathopoulou, M., & Cartalis, C. (2013b). A comparative analysis of the urban web of the greater Athens agglomeration for the last 20 years period on the basis of landsat imagery. *Fresenius Environmental Bulletin*, 22, 2139–2144.

Chrysoulakis, N., Abrams, M., Feidas, H., & Velianitis, D. (2004a). Analysis of ASTER Multispectral Stereo Imagery to Produce DEM and Land Cover Databases for Greek Islands: The REALDEMS Project. In: Prastacos, P., Cortes, U., De Leon, J. L., Murillo, M. (Eds), Proceedings of e-Environment: Progress and Challenge, 411–424.

Chrysoulakis, N., Diamandakis, M., & Prastacos, P. (2004b). GIS Based Estimation and Mapping of Local Level Daily Irradiation on Inclined Surfaces. In: Toppen, F. and P. Prastacos (Eds), Proceedings of the 7th AGILE Conference on Geographic Information Science, 587–597.

Chrysoulakis, N., & Cartalis, C. (2002). Improving the estimation of land surface temperature for the region of Greece: adjustment of a split window algorithm to account for the distribution of precipitable water. *International Journal of Remote Sensing*, 23, 871–880.

Dousset, B., & Gourmelon, F. (2003). Satellite multi-sensor data analysis of urban surface temperatures and landcover. *Journal of Photogrammetry and Remote Sensing*, 58, 43–54.

Enderle, D., & Weih, R. (2005). Integrating supervised and unsupervised classification methods to develop a more accurate land cover classification. *Journal of the Arkansas Academy of Science*, 59, 65–73.

Esch, T., Taubenböck, H., Chrysoulakis, N., Düzgün, H. S., Tal, A., Feigenwinter, C., & Parlow, E. (2013). Exploiting Earth Observation in Sustainable Urban Planning and Management - the GEOURBAN Project. In: Proceeding of Joint Urban Remote Sensing Event JURSE 2013, Sao Paulo, Brazil, April 21–23.

Fujisada, H. (1998). ASTER level-1 data processing algorithm. *IEEE Transactions on Geoscience and Remote Sensing*, 36, 1101–1112.

Fujisada, H. (1994). Overview of ASTER instrument on EOS-AM1 platform. In: Proceedings of SPIE, 2268, 14–36.

Grimmond, C. S. B., Roth, M., Oke, T. R., Au, Y. C., Best, M., Bettse, R., Carmichael, G., Cleugh, H., Dabberdt, W., Emmanuel, R., Freitas, E., Fortuniak, K., Hannal, S., Kleinm, P., Kalkstein, L. S., Liu, C. H., Nickson, A., Pearlmutter, D., Sailor, D., and Voogt, J. (2010). Climate and more sustainable cities: climate information for improved planning and management of cities (producers/capabilities perspective). *Procedia Environmental Sciences*, 1, 247–274.

Herold, M., Gardner, M., & Roberts, D. A. (2003). Spectral resolution requirements for mapping urban areas. *IEEE Transactions on Geoscience and Remote Sensing*, 41, 1907–1919.

Hung, T., Uchihama, D., Ochi, S., & Yasuoka, Y. (2006). Assessment with satellite data of the urban heat island effects in Asian mega cities. *International Journal of Applied Earth Observation and Geoinformation*, 8, 34–48.

Jiménez-Muñoz, J. C. & Sobrino, J. A. (2003). A generalized single-channel method for retrieving land surface temperature from remote sensing data. *Journal of Geophysical Research*, 108 (D22), 4688, doi:10.1029/2003JD003480

Liang, S. (2001). Narrowband to broadband conversions of land surface albedo: I. Formulae. *Remote Sensing for Environmental Sciences*, 76, 213–238.

Lo, C. P., & Quattrochi, D. A. (2003). Land-use and land-cover change, urban heat island phenomenon, and health implications: a remote sensing approach. *Photogrammetric Engineering and Remote Sensing*, 69, 1053–1063.

Lucht, W., Schaaf, C. B., & Strahler, A. (2000). An algorithm for the retrieval of albedo from space using semiempirical BRDF models. *IEEE Transactions on Geoscience and Remote Sensing*, 38, 977–998.

Mitraka, Z., Chrysoulakis, N., Kamarianakis, Y., Partsinevelos, P., & Tsouchlaraki, A. (2012). Improving the estimation of urban surface emissivity based on sub-pixel classification of high resolution satellite imagery. *Remote Sensing of Environment*, 117, 125–134.

Nichol, J. E. (1996). High-resolution surface temperature patterns related to urban morphology in a tropical city: a satellite-based study. *Journal of Applied Meteorology*, 35, 135−146.

Nikolakopoulos, K., Kamaratakis, E., & Chrysoulakis, N. (2006). SRTM vs ASTER elevation products. Comparison for two regions in Crete, Greece. *International Journal of Remote Sensing*, 27, 4819–4838.

Pauleit, S., & Duhme, F. (2000). Assessing the environmental performance of land cover types for urban planning. *Landscape and Urban Planning*, 52, 1–20.

Prata, A., Caselles, V., Coll, C., Ottle, C., & Sorbino, J. (1995). Thermal remote sensing of land surface temperature from satellites: current status and future prospects. *Remote Sensing Reviews*, 12, 175–224.

Qian, J.-H. (2007). Application of a variable-resolution stretched grid to a regional atmospheric model with physics parameterization. *Advances in Earth Science*, 22, 1185–1190.

Ranasinghe, A. (2008). Multi scale segmentation techniques in object oriented image analysis. Asian Conference on Remote Sensing ACRS 2008, Colombo, Sri Lanka.

Salisbury, J. W., D'Aria, D. M., & Wald, A. (1994). Measurements of thermal infrared spectral reflectance of frost, snow, and ice. *Journal of Geophysics Research*, 99, 24,235–24,240.

Salisbury, J. W., & D'Aria, D. M. (1994). Emissivity of terrestrial materials in the 3–5 μm atmospheric window. *Remote Sensing of Environment*, 47, 345–361.

Salisbury, W., & D' Aria, D. M. (1992). Emissivity of terrestrial materials in the 8–14 mm atmospheric window. *Remote Sensing of Environment*, 42, 83–106.

Santamouris, M., Synnefa, A., & Karlessi, T. (2011). Using advanced cool materials in the urban built environment to mitigate heat islands and improve thermal conditions. *Solar Energy*, 85, 3085–3102.

Schaaf, C. B., Gao, F., Strahler, A. H., Lucht, W., Li, X. W., Tsang, T., Strugnell, N. C., Zhang, X. Y., Jin, Y. F., Muller, J. P., Lewis, P., Barnsley, M., Hobson, P., Disney, M., Roberts, G., Dunderdale, M., Doll, C., d'Entremont, R. P., Hu, B. X., Liang, S. L., Privette, J. L., & Roy, D. (2002). First operational BRDF, albedo nadir reflectance products from MODIS. *Remote Sensing of Environment*, 83, 135–148.

Snyder, W. C., Wan, Z., Zhang, Y., & Feng, Y.-Z. (1998). Classification-based emissivity for land surface temperature measurement from space. *International Journal of Remote Sensing*, 19, 2753–2774.

Snyder, W. C., & Wan, Z., (1998). BRDF models to predict spectral reflectance and emissivity in the thermal infrared. *IEEE Transactions on Geoscience and Remote Sensing*, 36, 214–225.

Snyder, W. C., Wan, Z., Zhang, Y., & Feng, Y. (1997). Thermal infrared (3±14 μm) bidirectional reflectance measurements of sands and soils. *Remote Sensing of Environment*, 60, 101–109.

Sobrino, J. A., and Jiménez-Muñoz, J. C. (2005). Land surface temperature retrieval from thermal IR data: an assessment in the context of the Surface Processes and Ecosystem Changes through Response Analysis (SPECTRA) mission. *Journal of Geophysical Research*, 110, D16103, doi:10.1029/2004JD005588.

Stathopoulou, M., Synnefa, A., Cartalis, C., Santamouris, M., Karlessi, T., & Akbari, H. (2009). A surface heat island study of Athens using high-resolution satellite imagery and measurements of the optical and thermal properties of commonly used building and paving materials. *International Journal of Sustainable Energy*, 28, 59–76.

Stathopoulou, M., & Cartalis, C. (2009). Downscaling AVHRR land surface temperatures for improved surface urban heat island intensity estimation. *Remote Sensing of Environment*, 113, 2592–2605.
Stathopoulou, M., & Cartalis, C. (2007a). Study of the Urban Heat Island of Athens, Greece During Daytime and Night-time. In: IEEE Conference Proceedings of the 2007 Urban Remote Sensing Joint Event, Paris, France, 11–13 April 2007 (pp. 1−7).
Stathopoulou M., & Cartalis C. (2007b). Daytime urban heat island from Landsat ETM+ and Corine land cover. *Solar Energy*, 81, 358–368.
Stathopoulou, M., Cartalis, C., & Chrysoulakis, N. (2006). Using midday surface temperature to estimate cooling degree-days from NOAA-AVHRR thermal infrared data: an application for Athens, Greece. *Solar Energy*, 80, 414–422.
Stathopoulou, M., Cartalis, C., Keramitsoglou, I., & Santamouris, M. (2005). Thermal Remote Sensing of Thom's Discomfort Index (DI): Comparison with *In Situ* Measurements. In: Proceedings of the Remote Sensing 2005 Symposium (SPIE 2005), Brugge, Belgium, 19 September 2005.
Stathopoulou, M., Cartalis, C., & Keramitsoglou, I. (2004). Mapping micro-urban heat islands using NOAA/AVHRR images and CORINE land cover: an application to coastal cities of Greece. *International Journal of Remote Sensing*, 25, 2301–2316.
Streutker, D. R. (2002). A remote sensing study of the urban heat island of Houston, Texas. *International Journal of Remote Sensing*, 23, 2595–2608.
Tomlinson, C. J., Chapman, L., Thornes, J. E., & Baker, C. J. (2012). Derivation of Birminghams summer surface urban heat island from MODIS satellite images. *International Journal of Climatology*, 32, 214–224.
Toutin, T. (2008). ASTER DEMs for geomatic and geoscientific applications: a review. Elevation Modelling from Satellite VIR Data: A Review. *International Journal of Remote Sensing*, 29, 1855–1875.
Toutin, T. (2004). Geometric processing of remote sensing images: models, algorithms and method. *International Journal of Remote Sensing*, 25, 1893–1924.
Toutin, T. (2001). Elevation Modelling from Satellite VIR Data: A Review. *International Journal of Remote Sensing*, 22, 1097–1125.
Voogt, J. A., & Oke, T. R. (1998). Effects of urban surface geometry on remotely-sensed surface temperature. *International Journal of Remote Sensing*, 19, 895–920.
Weber, C., Petropoulou, C., & Hirsch, J. (2005). Urban development in the Athens metropolitan area using remote sensing data with supervised analysis and GIS. *International Journal of Remote Sensing*, 26, 785–796.
Whiteside, T., & Ahmad, W. (2005). A Comparison of Object-Oriented and Pixel-Based Classification Methods for Mapping Land Cover in Northern Australia. In: Proceedings of SSC2005 Spatial Intelligence, Innovation and Praxis: The National Biennial Conference of the Spatial Sciences Institute, Melbourne, Australia, pp. 1225–1231.
Wu, C., (2004). Normalized spectral mixture analysis for monitoring urban composition using ETM+ imagery. *Remote Sensing of Environment*, 93, 480–492.
Yamaguchi, Y., Kahle, A., Tsu, H., Kawakami, T., & Pniel, M. (1998). Overview of advanced spaceborne thermal emission and reflection radiometer (ASTER). *IEEE Transactions on Geosciences and Remote Sensing*, 36, 1062–1071.